Newtonian and Non-Newtonian sediment fluid flow hydrodynamic runoff model

Nawa Raj Pradhan, Ph.D., US Army Corps of Engineers, Engineer Research and Development Center, Coastal and Hydraulics Laboratory, Vicksburg, MS, Nawa.Pradhan@erdc.dren.mil
Ian Floyd, US Army Corps of Engineers, Engineer Research and Development Center, Coastal and Hydraulics Laboratory, Vicksburg, MS, Ian.E.Floyd@erdc.dren.mil
Charles Downer, Ph.D., US Army Corps of Engineers, Engineer Research and Development Center, Coastal and Hydraulics Laboratory, Vicksburg, MS, Charles.W.Downer@erdc.dren.mil
Stanford Gibson, Ph.D., US Army Corps of Engineers, Hydrologic Engineering Center, Davis, CA, Stanford.Gibson@erdc.dren.mil
Ronald Heath, US Army Corps of Engineers, Engineer Research and Development Center, Coastal and Hydraulics Laboratory, Vicksburg, MS, Ronald.E.Heath@erdc.dren.mil

Abstract

Assumption of Newtonian fluid flow condition, linear stress-strain relationship, fails for sediment laden fluids with higher volumetric sediment concentrations. As sediment concentrations increase, they begin to affect the fluid properties which alter the stress-strain relationship. In this study we developed the debris library, DebrisLib, that assigns a stress-strain relationship under non-Newtonian sediment-laden fluid flow conditions. This study also developed a linkage architecture to pass the hydrodynamic information to the non-Newtonian sediment dynamic subroutines and then returns the non-Newtonian sediment dynamic information. The Gridded Surface Subsurface Hydrologic Analysis (GSSHA) model is deployed as the hydrodynamic model. GSSHA-computed flow velocity, depth and concentration is passed to non-Newtonian sediment dynamic subroutines where internal shear stresses are computed and returned back to GSSHA. Using the volumetric sediment concentration, the Newtonian and non-Newtonian sediment fluid flow was tested in a 2D hydrodynamic runoff digital flume model. This test case of digital flume model overland simulation showed that mixed density and viscous fluid shear stress is significantly underestimated if a non-Newtonian condition is ignored. This under estimation of shear stress would significantly underestimate the sediment yield.

Introduction

Estimates of sediment graphs associated with hydrographs are essential for producing sediment yield estimates for designing efficient sediment control structures and for water quality

predictions. Physics-based distributed prediction of erosion and deposition of sediment is significant for not only long-term local geomorphological and landform changes point of view but also for better understanding of the land surface process and sediment sourcing and sinking mechanisms and its impact on hydrology, ecosystem, transport system, environment and socio-economy. Land use change and soil physical and chemical properties change also leads to the change in sediment sourcing, sinking and transport mechanism. One of the natural and/or man-made causes that brings about such changes in land use and soil property is wildfires. A rainfall event after a wildfire triggers a hyperconcentrated mud and debris flow. Such events with high concentration of sediment also changes the sediment laden water flow properties. The prime change of such water flow property is a non-linear shift of the viscosity which ultimately makes the water flow condition non-Newtonian.

Assumption of Newtonian fluid flow condition, defined by a linear stress-strain relationship, fails for sediment laden fluids with higher volumetric sediment concentrations. As sediment concentrations increase they begin to affect the fluid properties which alter the stress-strain relationship. Debris flows depart from linear stress-strain with no intercept assumptions embedded in the clear water flow equations. In this study, we developed the debris library, DebrisLib, that assigns a stress-strain relationship under non-Newtonian sediment laden fluid flow conditions (Pradhan et al., 2018; Floyd et al., 2019). This study also developed a general linkage architecture to pass the hydrodynamic information to the non-Newtonian sediment dynamic subroutines and then return non-Newtonian sediment dynamic information. The GSSHA model is deployed as the hydrodynamic model in this study. The GSSHA model is a fully-coupled overland/in-stream sediment transport (Newtonian flow regime) hydrodynamic model (Downer et al., 2015; Pradhan et al., 2018). GSSHA-computed flow velocity, depth and concentration is passed to non-Newtonian sediment dynamic subroutines where internal shear stresses are computed and passed back to GSSHA (Pradhan et al., 2018). Based on the volumetric sediment concentration, the Newtonian and non-Newtonian sediment fluid flow was tested in a 2D hydrodynamic runoff digital flume model.

Methodolody

The following steps were implemented as a method to develop the non-Newtonian sediment fluid flow dynamics capability in the parent hydrodynamic model:

a) The non-Newtonian processes were identified and coded as subroutines / functions.
b) The non-Newtonian process functions were arranged in the parent overland hydrodynamic code to align in correct order with other Newtonian and hydrodynamic processes. This arrangement and code development (in the two-dimensional overland sediment hydrodynamic GSSHA model) followed the linkage architecture
c) A test case, two-dimensional overland flume GSSHA model, was developed to make basic initial non-Newtonian internal shear stress function tests.

Details of the methodology are provided in the following sections.

Overland Sediment Detachment

Soil detachment can occur due to rainfall and overland flow. Total detachment is comprised of the sum of rainfall and overland flow detachment. Detachment by raindrops is considered to be a function of rainfall momentum, which is related to rainfall intensity (Downer et al., 2015). In this study, the analysis of the Newtonian and Non-Newtonian sediment transport mechanism is based on the flow shear stress. Flow shear stress falls under the surface runoff detachment mechanism.

Detachment by Surface Runoff: Surface runoff detaches soil particles by exerting a shear stress that breaks the bonds between soil particles. Erosion in rills is lumped and described as gross rill erosion. Within a grid cell rill erosion and flow within rills are assumed to be uniformly distributed. The detachment capacity rate by surface runoff has the form

$$D_c = a(\tau - \tau_{cr})^b \left(1 - \frac{G}{T_c}\right) \quad (1)$$

where

D_c = detachment capacity rate (kg $m^{-2} \cdot s^{-1}$),
a,b = empirical coefficients
τ = the flow shear stress (Pa)
τ_{cr} = the critical shear stress (Pa)
G = the sediment load (kg m^{-2} s^{-1})
T_c = the sediment transport capacity of surface runoff (kg m^{-2} s^{-1})

Shear stress in Newtonian Flow: Most hydraulic and sediment transport simulations assume that the transporting fluid has "Newtonian" properties. A Newtonian Fluid has two properties 1) a linear stress-strain relationship (Figure 1), and 2) that has a zero intercept (Figure 1).

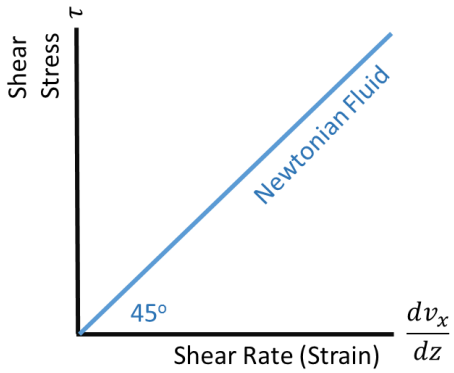

Figure 1. Model of Newtonian Fluids, which have a linear stress strain ratio and a stress-strain intercept of zero.

These Newtonian flow properties are appropriate for most fluids, including sediment laden fluids with lower volumetric concentrations, 16-530 g/l (Costa, 1988; Hessel, 2002).

Clear water flow resisting force is the boundary friction force and the boundary shear stress employed in the Newtonian flow condition is defined as:

$$\boldsymbol{\tau = \gamma R S_f} \qquad (2)$$

where

γ = the specific weight of water (Nm^{-3})
R = the hydraulic radius (m)
S_f = the friction slope

As sediment concentrations increase, they begin to affect the fluid properties, which alter the stress-strain relationship. Along with the primary boundary frictional force, these internal forces are resisting force due to viscosity, resisting force due to particle collision, and resisting force due to inter-particle friction. In general, as concentration increases (and the solid component coarsens) and internal shear stresses develop, the fluid crosses the Newtonian flow boundary and go through non-Newtonian flow regimes classified as:

(a) Hyperconcentrated Flow
(b) Mudflow
(c) Grain Flow
(d) Debris Flow,

The respective component of the total shear stress, $\boldsymbol{\tau}$, are
(a) yield shear stress + viscous shear stress, $\boldsymbol{\tau_{yield} + \tau_{viscous}}$
(b) turbulent shear stress, $\boldsymbol{\tau_{turbulent}}$
(c) dispersion shear stress, $\boldsymbol{\tau_{dispersive}}$ and
(d) internal friction dominated shear stress, $\boldsymbol{\tau_{Mohr-Coulomb}}$
The combination of the shear stress in non-Newtonian flow is defined as (O'Brien, J.S., and Julien, P.Y. 1985):

$$\boldsymbol{\tau = \tau_{yield} + \tau_{viscous} + \tau_{turbulent} + \tau_{dispersive} + \tau_{Mohr-Coulomb}} \qquad (3)$$

Figure 2 is the Newtonian fluid rheological plots where Figure 2a is the $\boldsymbol{\tau_{yield} + \tau_{viscous}}$ plot with the shear strain, Figure 2b is the $\boldsymbol{\tau_{yield} + \tau_{viscous}}$ + ($\boldsymbol{\tau_{turbulent}}$ *and or* $\boldsymbol{\tau_{dispersive}}$) plot with the shear strain. The last term on the right-hand side of equation 3 defines the pseudoplastics fluid which display the opposite properties of dilatant fluid shown in Figure 2c. This study is focused on the shear stress that falls on the rheological plots Figure 2a and Figure 2b.

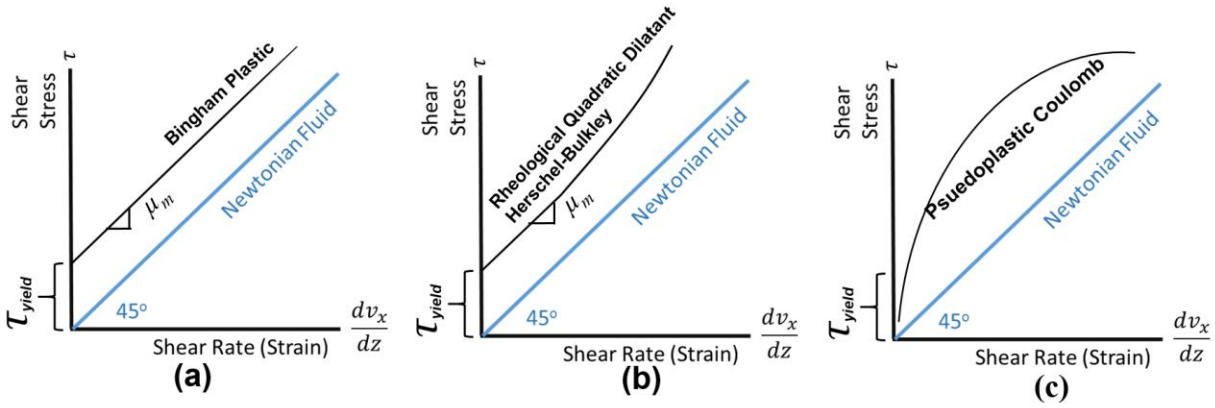

Figure 2. Newtonian fluid rheological plots**.**

From Equation 3 and Figure 2a, $\boldsymbol{\tau_{yield}}$ *and* $\boldsymbol{\tau_{viscous}}$ represent the intercept and the linear slope times the shear rate respectively in the hyperconcentrated fluid flow condition and the shear stress in this condition is defined as (Julian, 1995):

$$\boldsymbol{\tau_{hyperconcentrated}} = \boldsymbol{\tau_{yield}} + \boldsymbol{\mu_m}\left(\frac{\boldsymbol{dv_x}}{\boldsymbol{dz}}\right) = \boldsymbol{\tau_{yield}} + \boldsymbol{\mu_m}\left(\frac{\boldsymbol{3\bar{u}}}{\boldsymbol{h}}\right) \qquad (4)$$

where

$\boldsymbol{\mu_m}$ = the viscosity of the mixture (kg $m^{-1}S^{-1}$)
τ_{yield} = the critical shear stress (Pa)
v_x = fluid layer velocity (ms^{-1})
z = distance between fluid layers (m)
h = depth of water (m)
$\bar{u}$ = effective flow velocity

The turbulent shear is a second order (quadratic) term, making the stress-strain relationship non-linear as shown in Figure 2b, such that shear increases with the square of strain. From Equation 3 and Figure 2b, at rheological quadratic turbulent dilatant fluid stage, turbulent stress is added to hyperconcentrated stress as (Julian, 1995):

$$\boldsymbol{\tau_{hyperconcentrated}} + \boldsymbol{\tau_{turbulent}} = \boldsymbol{\tau_{hyperconcentrated}} + \boldsymbol{\rho_m l_m^2}\left(\frac{\boldsymbol{dv_x}}{\boldsymbol{dz}}\right)^2$$

$$= \boldsymbol{\tau_{hyperconcentrated}} + \boldsymbol{\rho_m l_m^2}\left(\frac{\boldsymbol{3\bar{u}}}{\boldsymbol{h}}\right)^2 \qquad \textbf{(5)}$$

where

ρ_m = the density of the mixture (kg m^{-3})
l_m = the Prandtl mixing length (Julien, 1995)

The diffusive shear is also a second order (quadratic) term, which is added to turbulent shear stress at higher concentration stage of sediment in the water. From Equation 3 and Figure 2b, at rheological quadratic diffusive dilatant fluid stage, diffusive stress is added to summation of hyperconcentrated stress and turbulent stress as (Julian, 1995):

$$\tau_{hyperconcentrated} + \tau_{turbulent} + \tau_{diffusive}$$

$$= \tau_{hyperconcentrated} + \tau_{turbulent} + C_{Bd}\rho_s \left(\left(\frac{0.615}{C_v} \right)^{1/3} - 1 \right)^{-2} d_s^2 \left(\frac{dv_x}{dz} \right)^2$$

$$= \tau_{hyperconcentrated} + \tau_{turbulent} + 0.01\rho_s \left(\left(\frac{0.615}{C_v} \right)^{1/3} - 1 \right)^{-2} d_s^2 \left(\frac{3\bar{u}}{h} \right)^2 \qquad (6)$$

where

C_{Bd} = an empirical parameter
$C_{Bd} \cong 0.01$ (Bagnold, 1954)
d_s = the particle diameter
ρ_s = particle density
C_v = the volumetric sediment concentration ranging from 0 to 1

Non-Newtonian Sediment Dynamics in a Hydrodynamic Model

Figure 3 represents the flow chart for a general linkage architecture of the non-Newtonian sediment laden fluid shear dynamics in a hydrodynamic model. Both for the overland and channel hydrodynamic and sediment dynamic model, first a threshold for non-Newtonian flow regime is identified with the calculation of a dimensionless parameter. Julian (1995) shows that the threshold for non-Newtonian flow regime is identified by the range of a viscous Parameter defined as:

$$\Pi_{viscous} = \frac{\tau - \tau_{yield}}{\mu_m \frac{dv_x}{dz}} = \frac{\tau - \tau_{yield}}{\mu_m \left(\frac{3\bar{u}}{h} \right)} \qquad (7)$$

where

μ_m = the viscosity of the mixture (kg $m^{-1}s^{-1}$)
τ_{yield} = the critical shear stress (Pa)
v_x = fluid layer velocity (ms^{-1})
z = distance between fluid layers (m)
h = depth of water (m)
$\bar{u}$ = effective flow velocity

$\Pi_{viscous} > 1$ employs the non-Newtonian flow, $1 < \Pi_{viscous} \leq 5 <$ is hyperconcentrated flow and $\Pi_{viscous} > 5$ defines the fluid flow conditions where additional stresses like turbulent and dispersive internal stresses are developed as shown in equation 6 and in Figure 2.
If the dimensionless parameter value falls in the non-Newtonian fluid flow, the fluid internal resistance shear stress is calculated as per equation 3 from the hydrodynamic flow information such as: velocity, depth of water and sediment concentration. The calculated non-Newtonian shear stress is then passed to the hydrodynamic model which estimates the sediment detachment capacity in equation 1. Also, this internal shear stresses of mud and debris flows can be deployed to estimate the hydraulic head slope of the sediment laden flow in equation 2.
Assumption of Newtonian fluid flow condition and a linear stress-strain relationship, fails for sediment laden fluids with higher volumetric sediment concentrations. As sediment concentrations increase they begin to affect the fluid properties which alter the stress-strain relationship. Debris flows depart from linear stress-strain assumptions with no intercept embedded in the clear water flow equations. In this study we developed the debris library that assigns a stress-strain relationship under non-Newtonian sediment-laden fluid flow condition (Pradhan et al., 2018; Floyd et al., 2019).

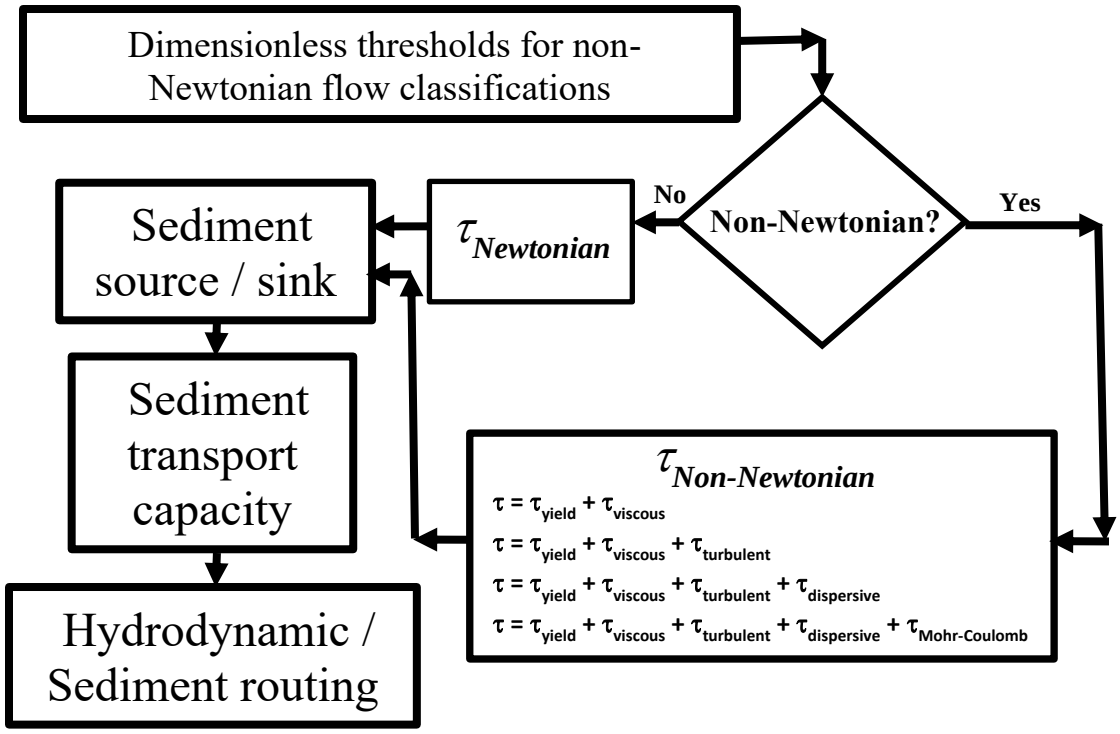

Figure 3. Linking hydrodynamics with non-Newtonian sediment fluid flow dynamics

Figure 4 shows a linkage architecture developed by this study to pass overland and channel hydrodynamic information to the non-Newtonian sediment dynamic subroutines, DebrisLib, and then to return non-Newtonian sediment dynamic information. GSSHA hydrodynamic model was deployed as overland and channel hydrodynamics shown in Figure 4. GSSHA model

is a fully coupled overland/in-stream and lake sediment transport (Newtonian flow regime) hydrodynamic model (Downer et al., 2015; Pradhan et al., 2018). In this study, GSSHA computed flow velocity, depth and concentration is passed to non-Newtonian sediment dynamic subroutines where internal shear stresses are computed and passed back to GSSHA (Pradhan et al., 2018). Although Figure 4 shows both the overland and in-stream non-Newtonian sediment flow dynamics linkage architecture in the hydrodynamics model, this study presents only the overland non-Newtonian sediment laden fluid flow condition.

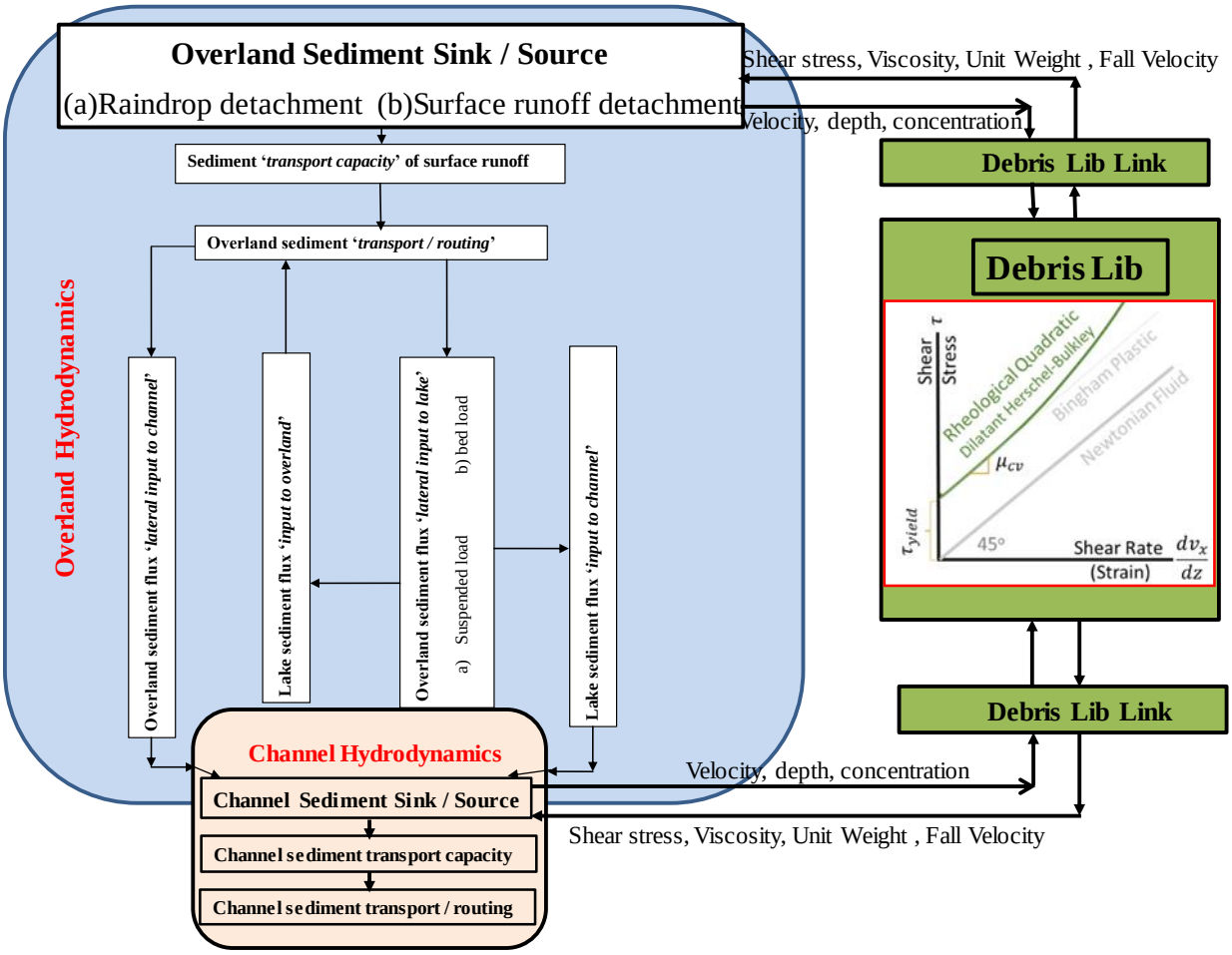

Figure 4. Linking non-Newtonian sediment fluid flow dynamics in a hydrodynamics model.

Test Case Model Development

For this study a simple linkage model was developed which includes:
(a) the non-Newtonian flow regime identification employing equation 7,
(b) passing of flow velocity, flow depth and the sediment concentration to non-Newtonian subroutines from the hydrodynamics model under non-Newtonian condition,

(c) calculation of the respective non-Newtonian shear stress employing equations 3 through equation 6, and
(d) calculation of the detachment capacity in equation 1using the non-Newtonian shear stress for each grid under non-Newtonian condition.
A gridded digital flume model was developed as shown in Figure 5 to test the Newtonian and non-Newtonian shear stress that would develop for sediment sourcing force. The contrived model included a uniform precipitation, two-dimensional overland flow and overland sediment erosion processes (Downer et al., 2015). Figure 5a shows the length and the slope of the flume which is based on the USGS debris flow flume (Iverson, 2010). Figure 5b shows the plan view of the GSSHA flume model where the elevations are hypothetically adjusted to maintain the slope defined by Figure 5a. The grid resolution of the GSSHA flume model in Figure 5b is two meters, which is also the width of the flume. Figure 5c shows the two-dimensional flow vector of the overland flume model.

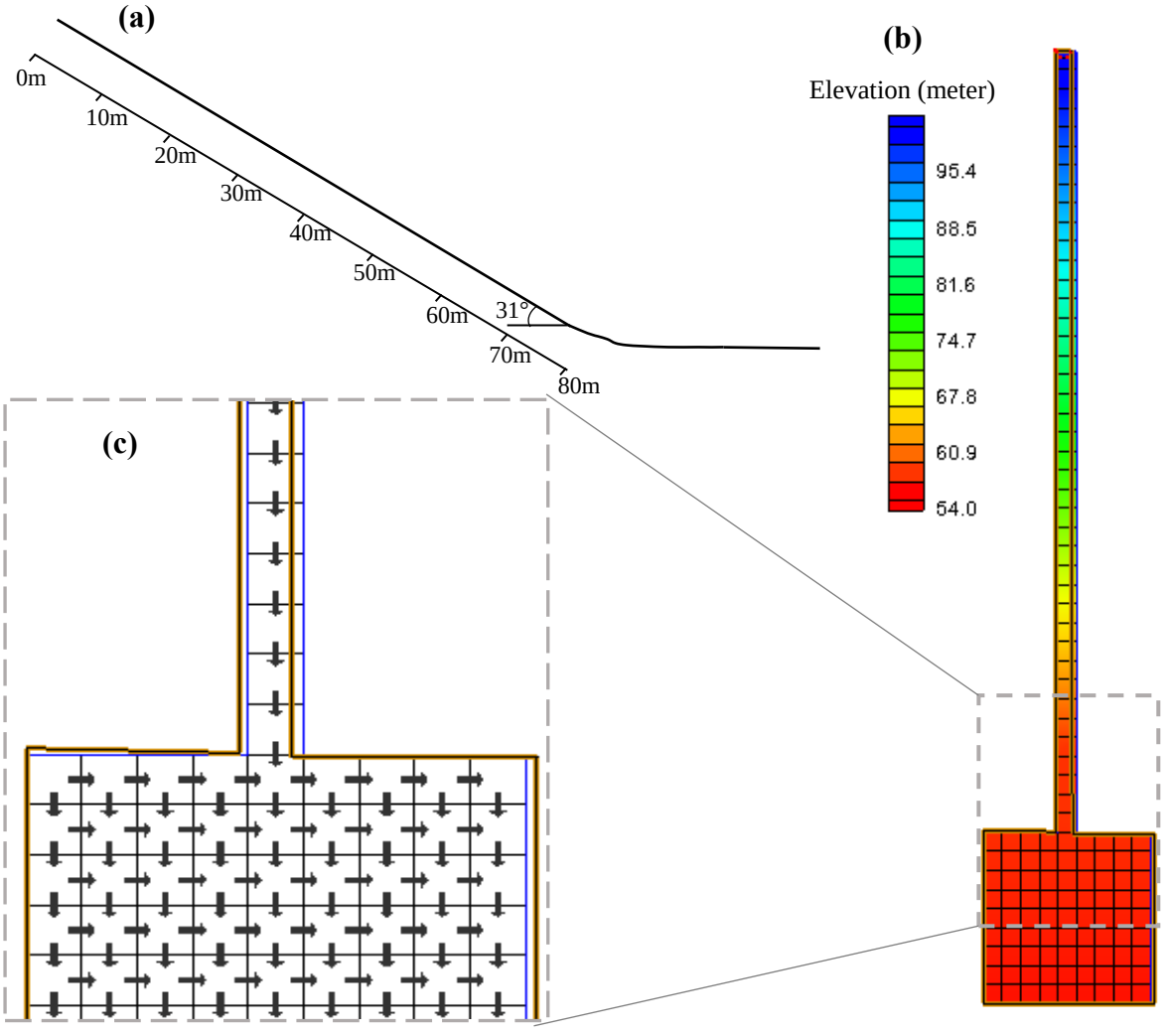

Figure 5. A gridded digital flume model: (a) side view with the length and the slope of the flume (b) Plan view with elevation of the GSSHA flume model (c) two-dimensional overland flow vector.

Results and Discussion

Based on the volumetric sediment concentration, the Newtonian and non-Newtonian sediment fluid flow was tested in 2D hydrodynamic runoff digital model. A sediment concentration boundary condition of 0.05 m^3m^{-3} was deployed at the beginning of the flume (0 m of Figure 5a). This sediment concentration was gradually increased until the hyperconcentration stage was reached as shown by equation 4 and Figure 2a. The total shear stress (yield shear stress + viscous shear stress) was calculated employing equation 4. At the hyperconcentrated stage, Newton boundary shear stress, defined by equation 2, was also calculated as to compare the difference in magnitude of shear stress, if the Newtonian assumptions are employed even when the non-Newtonian condition already existed. Figure 6 shows a huge difference in the magnitude of non-Newtonian and Newtonian shear stress. Figure 6 shows that shear stress is significantly underestimated if a non-Newtonian condition is ignored. This underestimation of shear stress would underestimate the sediment yield predictions unless unrealistic parameter values and initial conditions are imposed during the calibration process. The boundary sediment concentration was further increased until a turbulent shear condition was identified with the dimensionless parameter value defined by equation 7. Figure 6 shows this turbulent shear stress added to the hyperconcentrated shear stress in shear thickening fluid or dilatant condition. The result could be different from Figure 6 for shear thinning, pseudo plastic condition, which is yet to be tested.

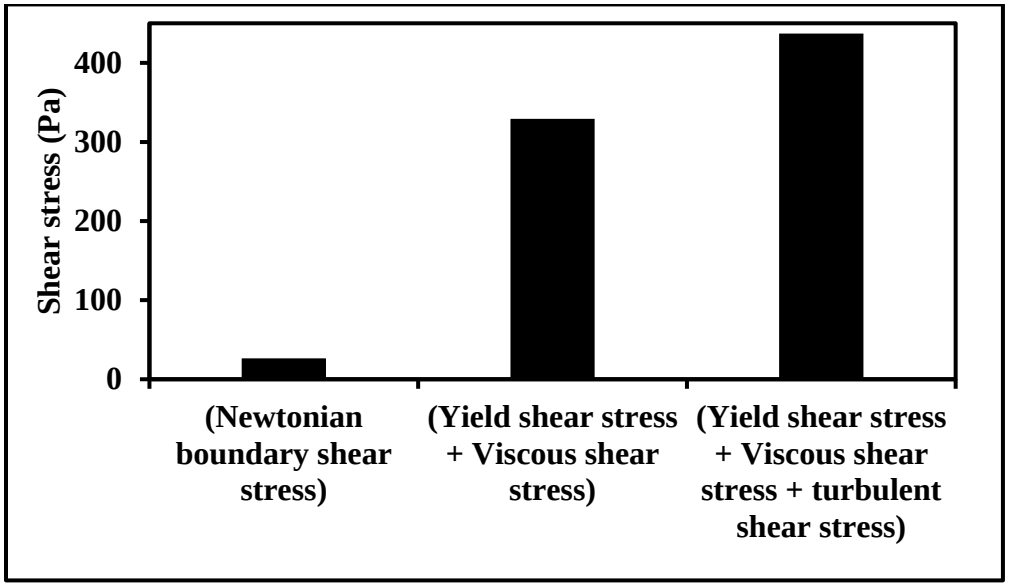

Figure 6. A comparison of simulated non-Newtonian total shear stresses with the Newtonian shear stress under non-Newtonian condition.

In Equation 4, yield stress, τ_{yield} , is empirically defined. Yield stress (O'Brian and Julian, 1985; Julian, 1995) is defined as:

$$\tau_{yield} = ae^{b*C_v} \quad (8)$$

The yield stress equation has two user-specified parameters, a linear coefficient 'a' and exponential multiplier of the concentration 'b'. Julian (1995) provides Table 1 to guide parameter selection:

Table 1. Yield stress parameters from Julian (1995)

Material	**a**	**b**
"Typical soil"	0.005	7.5
Kaolinite	0.05	9
Sensitive Clays	0.03	10
Bentonite	0.002	100

Most of these empirical relationships are derived from laboratory scale physical models. Fitting of the 'a' and 'b' parameter values listed in Table 1 was performed in the virtual laboratory digital flume model. Costa (1988) specifies the dirty water concentration for non-Newtonian /Newtonian flows as shown in Table 2.

Table 2. Dirty water concentration (g/l) of different types of flow (based on Costa, 1988; Hessel, 2002)

Normal stream flow concentration (g/l)	Hyperconcentrated flow concentration (g/l)	Debris flow concentration (g/l)
16-530	530-1285	1285-2088

Table 2 shows that approximately 50% or 0.5 m^3m^{-3} of concentration would transition the Newtonian flow towards non-Newtonian fluid flow condition. Therefore, 50% concentration was used as a boundary condition in the flume model. 'a' and 'b' parameter values were adjusted by employing this boundary concentration in Equation 8 so that the viscous parameter defined by Equation 8 fell within the flow condition defined in Table 2. This process resulted parameter value of a = 0.03 and that for b = 18.9 for this test case. Figure 6 was analyzed based on this identified values of 'a' and 'b'.

Conclusion

Newtonian fluid flow condition with linear stress-strain relationship are not applicable for sediment-laden fluids with high volumetric sediment concentrations. As sediment concentrations increase, they begin to affect the fluid properties, which alter the stress-strain relationship. In this study, the debris library was developed that calculates a stress-strain relationship under non-Newtonian sediment laden fluid flow conditions. This study also developed a linkage architecture to relate the hydrodynamic information to the non-Newtonian sediment dynamic subroutines and return the non-Newtonian sediment dynamic information to

the hydrodynamic parent code. The Gridded Surface Subsurface Hydrologic Analysis (GSSHA) model is deployed as the hydrodynamic model. GSSHA-computed flow velocity, depth and concentration information is linked to non-Newtonian sediment dynamic subroutines. The non-Newtonian sediment dynamic subroutines computed the internal shear stresses which are returned to GSSHA. Based on the volumetric sediment concentration, the Newtonian and non-Newtonian sediment fluid flows were tested in a 2D hydrodynamic runoff digital flume model. 2D overland simulation of this test case digital flume model showed that mixed density viscous fluid shear stress is significantly underestimated if a non-Newtonian conditions are ignored. This underestimation of shear stress would therefore significantly underestimate the sediment yield. In this initial phase of the coupling and testing research and development effort, the result analysis is limited only to the internal resisting shear stress of the overland flow process. The research and development effort so far includes:

1) Development of the non-Newtonian sediment dynamics subroutines. We define these combined non-Newtonian sediment dynamics subroutines as DebrisLib and is still in progress.
2) Linkage of these non-Newtonian sediment dynamics subroutines with the overland hydrodynamics so that the linkage architecture represents the mathematical model of physically-based sediment and hydrodynamic processes aligned in order to calculate the internal shear stresses.
3) Development and numerical testing of a sediment hydrodynamic digital flume model for internal shear stresses calculations and to identify the parameter value ranges.

Development and coupling of the non-Newtonian overland sediment transport and routing mechanism in the overland hydrodynamic model is in progress. Development of the non-Newtonian fluid flow processes in the 1D instream hydrodynamic model will follow the 2D overland non-Newtonian fluid flow processes.

References

Bagnold, R.A. 1954. “Experiments on a gravity-free dispersion of large solid spheres in a Newtonian fluid under shear”, Proc. Roy. Soc. Lond. A225, 49-63.

Costa, J.E. 1988. “Rheologic, geomorphic, and sedimentologic differentiation of water floods, hyperconcentrated flows, and debris flows”, Chapter 7 in: Baker, V.R., R.C. Kochel & P.C. Patton (eds.) Flood Geomorphology. New York: Wiley, pp. 113-122

Downer, C.W., Pradhan, N.R., Ogden, F.L., and Byrd, A. 2015. “Testing the effects of detachment limits and transport capacity formulation on sediment runoff predictions using the US Army Corps of Engineers GSSHA model”, ASCE J. Hydrol. Eng., 10.1061/(ASCE)HE.1943-5584.0001104

Floyd, I.E., Gibson, S., Heath, R.E., Ramos-Villanueva, M., and Pradhan, N. 2019. “Development of 'Debris Library' and 1D HEC-RAS and 2D Adaptive Hydraulics Linkage-Architecture Post-Wildfire for non-Newtonian Flows”, submitted to Proc. SEDHYD 2019, Reno, NV.

Hessel, R. 2002. “Modelling soil erosion in a small catchment on the Chinese Loess Plateau. Applying LISEM in extreme conditions”, Netherlands Geographical Studies 307. KNAG: Utrecht, The Netherlands.

Iverson, R. M., Logan, M., LaHusen, R. G., and Berti, M. 2010. “The perfect debris flow? Aggregated results from 28 large-scale experiments”, J. Geophys. Res., 115, F03005, doi:10.1029/2009JF001514.

Julien, P.Y. 1995. Erosion and Sedimentation. Second edition, Cambridge University Press, Cambridge, UK.

O’Brien, J.S., and Julien, P.Y. 1985. “Physical properties and mechanics of hyperconcentrated sediment flows”, Proc. ASCE Specialty Conference on the Delineation of Landslide, Flashflood and Debris Flow Hazards, Utah Water Research Lab, Series UWRL/G-85/03, 260-79.

Pradhan, N.R., Floyd, I.E., Heath, R., Downer, C.W., and Gibson, Stanford. 2018. “Development of ‘Debris Library’ and ‘GSSHA’ linkage-architecture for non-Newtonian sediment fluid flow”, 2018 AGU Fall Meeting, Washington D.C., 10-14 December, Paper Number: EP21D-2277.